ISSN 0021-3640, JETP Letters, 2014, Vol. 100, No. 9, pp. 555–560. © Pleiades Publishing, Inc., 2014.
Original Russian Text © A.V. Melnikov, L.G. Eliseev, S.E. Lysenko, S.V. Perfilov, R.V. Shurygin, L.I. Krupnik, A.S. Kozachek, A.I. Smolyakov, 2014, published in Pis'ma v Zhurnal Eksperimental'noi i Teoreticheskoi Fiziki, 2014, Vol. 100, No. 9, pp. 633–638.

Radial Homogeneity of Geodesic Acoustic Modes in Ohmic Discharges with Low B in the T-10 Tokamak

A. V. Melnikov[a, b], L. G. Eliseev[a], S. E. Lysenko[a], S. V. Perfilov[a], R. V. Shurygin[a], L. I. Krupnik[c], A. S. Kozachek[c], and A. I. Smolyakov[a, d]

[a] *National Research Centre Kurchatov Institute, pl. Akademika Kurchatova 1, Moscow, 123182 Russia*
[b] *National Research Nuclear University MEPhI, Kashirskoe sh. 31, Moscow, 115409 Russia*
e-mail: melnikov_07@yahoo.com
[c] *Institute of Plasma Physics, National Scientific Center Kharkov Institute of Physics and Technology, Kharkov, 61108 Ukraine*
[d] *University of Saskatchewan, Saskatoon, SK S7N 5E2, Canada*

Received September 10, 2014; in final form, September 30, 2014

The electric potential oscillations in the hot plasma zone have been measured directly using a heavy ion beam probe at the frequencies of geodesic acoustic modes in the T-10 tokamak (the major and minor radii are $R =$ 1.5 m and $a = 0.3$ m, respectively, and the toroidal magnetic field is $B = 1.5$–2.5 T). In discharges with the lowered magnetic field $B = 1.55$ T, the diagnostic beam can probe a rather wide radial plasma region ($0.06 < r < 0.28$ m). This made it possible to study the radial structure of geodesic acoustic modes. It has been shown that the frequency and amplitude of geodesic acoustic modes in the region under study are constant over the radius in the whole region of observation. Thus, it has been shown experimentally that the observed frequency of geodesic acoustic modes may not correspond to the predictions of the local theory ($f \sim \sqrt{T_e}$) in a wide radial range comparable with the plasma minor radius. The numerical simulation of the turbulence dynamics using the solution of Braginskii magnetohydrodynamic equations for a peripheral plasma has showed the formation of geodesic acoustic modes in the observed frequency range owing to the nonlinear interaction between broadband turbulence modes.

DOI: 10.1134/S0021364014210103

INTRODUCTION

Toroidal systems of the tokamak type play the leading role in the current studies on nuclear fusion. In the 1970s, the neoclassical theory of the energy transport across the confined magnetic field was elaborated with allowance for pair collisions of particles in the toroidal magnetic geometry. According to this theory, being heated, a plasma may transfer to the collisionless regime, in which the transport coefficients decrease with the increase in the plasma temperature, i.e., the energy confinement is improved. However, it occurred that transport, particularly of the electron component, has an anomalous character and does not correspond to the neoclassical theory. Turbulent oscillations with different excitation mechanisms, amplitudes, frequencies, wavenumbers, and regions of spatial localization develop in plasma. Small-scale oscillations may combine into middle-scale and global modes forming the so-called inverse cascades of oscillation energy transport. Geodesic acoustic modes (GAMs), which are the high-frequency branch of zonal flows in the toroidal plasma, refer to these middle-scale modes.

The notion of zonal flow is widely used in the description of the turbulent processes in the atmospheres of the Earth and solar system planets. In meteorology, it means the directed flow coming from the west to the east along the latitude. In a tokamak, zonal flows are plasma torsional oscillations along the magnetic surfaces in the poloidal direction. Geodesic acoustic modes are the high-frequency (tens and hundreds of kilohertz) branch of the zonal flows. For the first time, geodesic acoustic modes having the electrostatic potential component with poloidal and toroidal numbers $m = n = 0$ and the plasma pressure component with $m = 1$ were introduced within the ideal magnetohydrodynamics model [1]. Geodesic acoustic modes are examples of the self-organization of the plasma excited by the low-frequency drift modes, in which the energy is pumped to longer wavelength oscillations owing to the modulation instability or inverse cascades. GAMs excited by fast electrons (EGAMs) were also found.

Geodesic acoustic modes are intensively studied as a possible mechanism of the self-regulation of plasma turbulence [2, 3], in which small-scale turbulence radially carrying the energy from the plasma to the wall transforms into torsional oscillations of GAMs con-

serving the energy in the plasma. In addition, the theory predicts that the transitions to the improved plasma confinement are accompanied by the complicated interaction between the edge small-scale turbulence, electric field, rotation shear (inhomogeneity), and zonal flows [4].

Recently, it was demonstrated that geodesic acoustic modes and Alfvén eigenmodes caused by beta (relative pressure) of plasma (BAE) having low but nonzero m and n values on the potential perturbations [5] have a common expression for the frequency:

$$f_{\mathrm{GAM/BAE}} = \frac{V_{T_i}}{2\pi R} \times \sqrt{\frac{7}{4} + \tau_e + q^{-2}\left(\frac{23}{2} + 8\tau_E + 2\tau_E^2\right)(7 + 4\tau_E)^{-1}}, \quad (1)$$

where $\tau_e = T_e/T_i$; $V_{T_i}^2 = 2T_i/m_i$; T_e and T_i are the electron and ionic temperature, respectively; m_i is the ion mass; and q is the safety factor [6, 7]. In the toroidal geometry, the ionic pressure perturbations caused by the toroidal compressibility are anisotropic, which gives an adiabatic index of 7/4 [8]. The second term τ_e in Eq. (1) is associated with the electron compressibility in the adiabatic limit $\omega \ll V_{T_e}/qR$. We note that the electron pressure perturbations cause the lateral oscillation band with $m = 1$. The multiplier $(7 + 4\tau_e)^{-1}$ at q^{-2} is associated with the longitudinal compressibility of the ionic and electron liquids (the same as for the planar ion-sound modes). Expression (1) describes the local spectrum (continuum), in which the local frequency $f_{\mathrm{GAM/BAE}}$ varies over the radius because T_e, T_i, and q are functions of $\rho = r/a$.

Experimental studies of the radial structure of geodesic acoustic modes performed on modern tokamaks give ambiguous results. On the TEXT [9] and FT-2 [10] tokamaks, the radius dependence of the frequency of geodesic acoustic modes was observed in accord with the predictions of the local theory given by Eq. (1). However, it was shown in experiments on the JFT-2M [11], HL-2A (where EGAM were studied) [12], ASDEX [13], TCV [14] and GLOBUS-M [15] facilities that the observed geodesic acoustic modes have an almost constant frequency in a certain finite radial region in which T_e changes noticeably, which does not agree with (1). We note that the observations of geodesic acoustic modes are a complicated diagnostic problem requiring the application of special highly sensitive diagnostics of the electrical field or plasma rotation. For this reason, each of the experiments mentioned above involved diagnostic limitations on the region of observation of geodesic acoustic modes, which did not make it possible to obtain a comprehensive answer to the question about the radial structure of geodesic acoustic modes. This answer was the aim of experiments at the T-10 tokamak, in which the measurements of geodesic acoustic modes of the plasma potential were performed in a wide radial interval. Their results are given in this work. They show that the frequency and amplitude of the oscillations may not change over the radius.

The article is organized as follows. First, the discharge parameters and the applied diagnostics are indicated. Then, the main results of experiments—radial dependences of the frequency and amplitude of geodesic acoustic modes—are given. After that, the numerical model of the edge turbulence is described in short and the calculation results are presented. The main results of the work are summarized in the last section.

EXPERIMENTAL CONDITIONS

In the T-10 circular tokamak ($R = 1.5$ m, $a = 0.3$ m, toroidal magnetic field $B = 1.5$–2.5 T), geodesic acoustic modes were studied using a heavy ion beam probe, correlation reflectometry, and Langmuir probes [3, 16, 17]. It was shown that the frequency of the mode f^{exp} varies with the temperature as $\sqrt{T}$ [3, 16]. This confirms that these modes are caused by the geodesic compressibility and belong to the GAM/BAE type.

To study the radial structure of geodesic acoustic modes, we used the method of heavy ion beam probe (HIBP), which is the unique direct method of measuring the electric potential in the hot plasma zone [18]. We applied the diagnostic beam of Tl^+ ions with the energy $E_1 < 180$ keV [19]. The probing primary beam moved through the plasma over the Larmor circle to the ionization point (SV). The secondary Tl^{++} ions with the energy E_2 moved over the circle with the radius half as large and got into the energy analyzer. The energy difference $\delta\varphi_{\mathrm{SV}} = E_1 - E_2$ made it possible to find the local potential value at the ionization point and its fluctuations. Varying the injection angle α and the primary beam energy, one can change the position of SV over the so-called detector grid (Fig. 1). In these experiments, we applied scanning of the position of SV over the cross section of the plasma using the variation of the voltage U_{sc} with a period of 10 ms. The plasma density profile n_e was measured by multichannel interferometers. The electron temperature T_e was estimated from the soft X-ray radiation (SXR) and the second harmonic of the electron–cyclotron emission (ECE). The central ionic temperature $T_i(0)$ was determined from the spectrum of charge-exchange neutrals. The diagnostics used are described in more detail in [20].

EXPERIMENTAL RESULTS

In this work, the regime with the lowered magnetic field $B = 1.55$ T was used that made it possible to

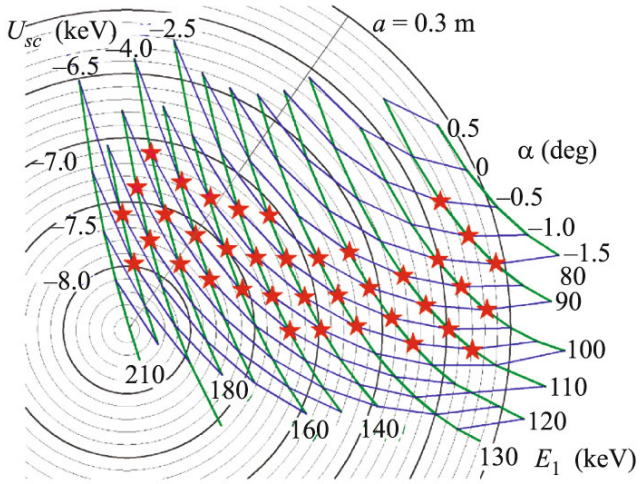

Fig. 1. (Color online) Detector grid for the heavy ion beam probe at the T-10 tokamak in the field $B = 1.5$ T obtained at the variation of the beam energy E_1 and the injection angle α (the voltage on the deflecting plates for scanning U_{sc}). Asterisks denote the available points of observation.

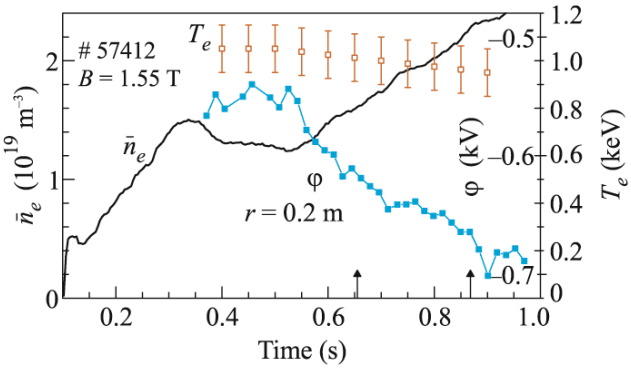

Fig. 2. (Color online) Evolution of the chord-averaged plasma density $\bar{n}_e$, local potential value φ (ρ = 0.67), and central electron temperature $T_e(0)$ in pulse no. 57412 with the increase in the density.

expand the region of observation by the method of heavy ion beam probe to the center of the plasma. In this regime, the heavy ion beam probe makes it possible to observe both the periphery (ρ = 0.7–1) and center (ρ ≥ 0.2) of the plasma. The studied regime with the ohmic plasma heating (the current I_p = 140 kA) is characterized by the low chord-averaged density $\bar{n}_e$ slowly changing from 1.3 to 2.4 × 10^{19} m^{-3} owing to the gas puffing. The time evolution of the main plasma parameters is shown in Fig. 2. It can be seen that with an increase in the density, the electron temperature decreases somewhat and the absolute value of the negative plasma potential increases. A geodesic acoustic mode is observed in the power spectrum of the plasma potential oscillations (PSD) as a characteristic sharp peak having a high contrast in comparison with the surrounding background of the broadband oscillations (Fig. 3). At considerable variation of the density $\bar{n}_e$ (from 1.8 to 2.4 × 10^{19} m^{-3}), the frequency of the mode decreases slightly, which corresponds to the weak square-root temperature dependence predicted by Eq. (1).

The radial distribution of the frequency of geodesic acoustic modes is shown in Fig. 4. Modes are not found outside the limiter beyond the radius r = 0.3 m. The mode frequency is almost constant in the region of observation (0.2 < ρ < 0.9), which is inconsistent with the calculation of $f_{GAM/BAE}$ by Eq. (1). The amplitude of geodesic acoustic modes is also almost constant over the radius (Fig. 5). Thus, it was shown that the geodesic acoustic mode in the studied regime has the properties of a global eigenmode. The existing theory [4, 5, 21] predicts such a possibility in the presence of a local maximum for $f_{GAM/BAE}$, which, however, is not implemented under the conditions of this experiment. The presence of the other type of eigenmodes, which do not require the local maximum $f_{GAM/BAE}$ for their existence, should also be noted [22]. Such modes can be formed in discharges with a monotonic temperature and positive shear of the magnetic field. Interestingly, the harmonic of the eigenfunctions with m = 0 in [21, 22] has a stepwise character, so that its amplitude remains constant in a considerable region over the radius. The amplitude step in [21] occurs near the maximum point and in [22] near the plasma column. For both types of solutions, the frequency of global eigenmodes exceeds the local frequency over the whole radial region. We note that the experimental frequency f^{exp} coincides with $f_{GAM/BAE}$ only in the periphery of the column (at ρ = 0.8–0.9) and it is noticeably lower in its other part (Fig. 4). The

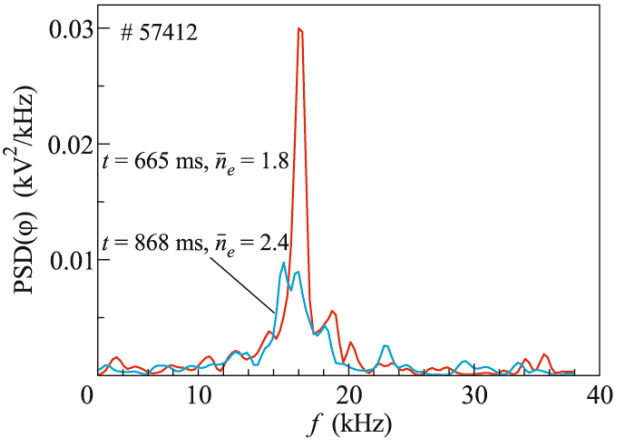

Fig. 3. (Color online) Spectra of potential oscillations in the regime with the increase in the density that are measured at time instants marked with arrows in Fig. 2. A slight decrease in the frequency of geodesic acoustic modes at the higher density is caused by the decrease in the electron temperature.

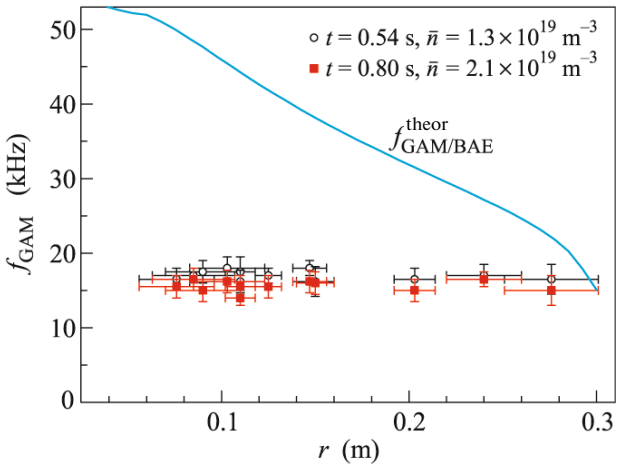

Fig. 4. (Color online) Radial distributions of the frequency of the peak of geodesic acoustic modes at different plasma densities. The solid curve corresponds to calculations of the frequency by Eq. (1). A slight decrease in the frequency of geodesic acoustic modes is caused by the temperature decrease with the increase in the density.

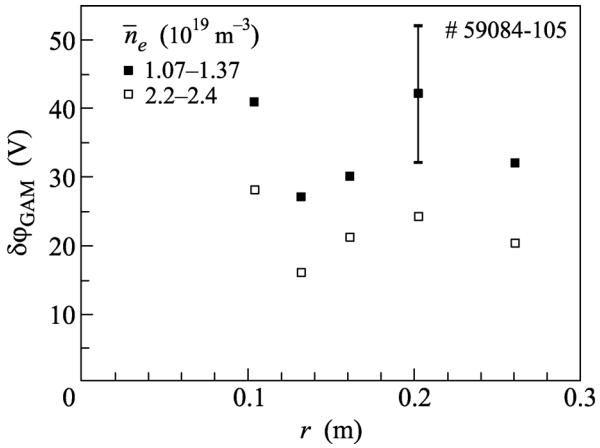

Fig. 5. Radial distribution of the amplitude of geodesic acoustic modes at different plasma densities.

latter may indicate the considerable role of the nonlinear processes in the generation of geodesic acoustic modes and the formation of global solutions. With an increase in the density, the frequency and amplitude decrease. At the densities exceeding $\bar{n}_e = 2.4 \times 10^{19}$ m^{-3}, the mode disappears. The weak decay of f^{exp} at the edge (at $\rho = 0.9$) observed at an increase in the density is in agreement with calculations of $f_{\text{GAM/BAE}}$ with allowance for a decrease in the temperatures T_e and T_i at the periphery.

NUMERICAL SIMULATION

As a rule, geodesic acoustic modes and zonal flows are considered within the linear theory [21, 22]. In this case, a number of effects associated with the influence of the nonlinear terms, which can be responsible for the global structure of geodesic acoustic modes, are lost. The nonlinear simulation of geodesic acoustic modes was performed using a five-field code (φ, n_e, p_e, p_i, $V_{\|i}$) capable of solving the nonlinear two-fluid Braginskii magnetohydrodynamic equations in toroidal geometry at the tokamak periphery ($0.8 < \rho < 1$) at the developed drift-resistive ballooning turbulence in the electrostatic approximation [23, 24]. Here, p_e and p_i are the pressures of electrons and ions, respectively, and $V_{\|i}$ is the longitudinal ion velocity.

The calculation showed that the nonlinear interaction between different spectral components under toroidal conditions leads to the appearance of specific high-frequency magnetohydrodynamic modes in the Fourier spectra, which are geodesic acoustic modes with the properties close to those observed in the experiment. It was also shown that, in addition to the turbulent Reynolds force, the Stringer–Winsor force associated with the total-pressure geodesic acoustic modes noticeably affects the poloidal rotation rate [24].

Figure 6 shows the calculated turbulent Fourier spectra of the amplitude of the fluctuations of (a) the electrostatic potential, (b) the density, and (c) the velocity of the zonal flow $V_{E\times B} = (c/B)d\varphi/dr$. The region near the frequency $(f_{\text{GAM}})^{\text{theor}} = 15$ kHz calculated by Eq. (1), where the characteristic spectral maxima are located, is shaded. It follows from the calculations that, under developed turbulence conditions, geodesic acoustic modes are not strictly coherent. They are manifested in the form of increased activity in a rather wide frequency range (~12–28 kHz), which differs somewhat from the experimental data having a narrower frequency peak in this range.

The calculations also showed that the frequency region of geodesic acoustic modes is shifted with an increase in T_e toward higher frequencies as $f \sim \sqrt{T_e}$ in agreement with experiments.

It follows from the results of the numerical simulation that satellite peaks in the region $f > (f_{\text{GAM}})^{\text{theor}}$ and in the region $f < (f_{\text{GAM}})^{\text{theor}}$ are always present in the frequency region of geodesic acoustic modes in addition to the peak $(f_{\text{GAM}})^{\text{theor}}$. The presence of the satellite peak of geodesic acoustic modes in the region $f > (f_{\text{GAM}})^{\text{theor}}$ corresponds to the results of the measurements [3, 16, 17]. A theoretical analysis of the appearance of the satellite oscillations has not yet been performed. Additional numerical calculations of the turbulent dynamics at different tokamak plasma parameters are needed for the understanding of the nature of these satellites using the experimental database on time Fourier spectra from different devices.

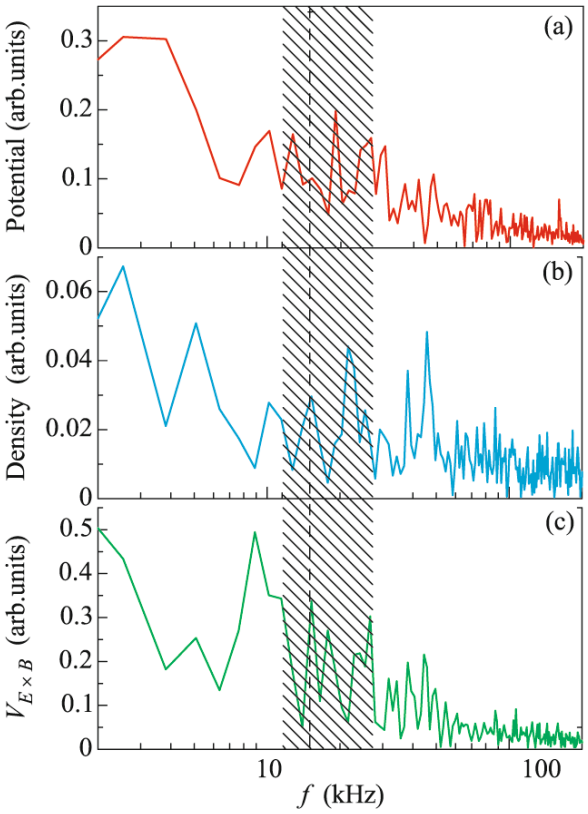

Fig. 6. (Color online) Amplitude Fourier spectra of (a) turbulent potential fluctuations, (b) density, and (c) zonal velocity. The region of the excitation of geodesic acoustic modes is shaded. The dashed line corresponds to the theoretical value $(f_{GAM})^{theor} = 15$ kHz.

CONCLUSIONS

For the first time, the oscillations of the plasma electric potential caused by geodesic acoustic modes were measured over almost the total radial interval $(0.2 < \rho < 0.9)$ in the ohmic regime of the T-10 tokamak at the lowered magnetic field $B = 1.55$ T using the heavy ion beam probe of the plasma. It has been shown that the frequency and amplitude of geodesic acoustic modes on the electric potential are constant over the radius within the experimental error. Thus, it has been demonstrated that the observed frequency of geodesic acoustic modes may not correspond to those predicted by the local theory assuming the strong radial inhomogeneity of the frequency owing to its square root dependence on the local temperature. The obtained results are the experimental confirmation of the existence of the global eigenmodes, the basic possibility of the existence of which is considered in the theory [22]. The numerical simulation of the dynamics of the turbulence by solving the Braginskii magnetohydrodynamic equations at the plasma periphery has indicated the possibility of the formation of geodesic acoustic modes owing to the nonlinear interaction between broadband turbulence modes near 15 kHz in qualitative agreement with the experiment.

We are grateful to the T-10 team for the help in performing the experiments. This work was supported by the Russian Science Foundation (project no. 14-22-00193).

REFERENCES

1. N. Winsor, J. L. Johnson, and J. M. Dawson, Phys. Fluids **11**, 2448 (1968).
2. A. Fujisawa, T. Ido, A. Shimizu, S. Okamura, K. Matsuoka, H. Iguchi, Y. Hamada, H. Nakano, S. Ohshima, K. Itoh, K. Hoshino, K. Shinohara, Y. Miura, Y. Nagashima, S.-I. Itoh, M. Shats, H. Xia, J. Q. Dong, L. W. Yan, K. J. Zhao, G. D. Conway, U. Stroth, A. V. Melnikov, L. G. Eliseev, S. E. Lysenko, S. V. Perfilov, C. Hidalgo, G. R. Tynan, C. Holland, P. H. Diamond, G. R. McKee, R. J. Fonck, D. K. Guptaand, and P. M. Schoch, Nucl. Fusion **47**, S718 (2007).
3. A. V. Melnikov, V. A. Vershkov, L. G. Eliseev, S. A. Grashin, A. V. Gudozhnik, L. I. Krupnik, S. E. Lysenko, V. A. Mavrin, S. V. Perfilov, D. A. Shelukhin, S. V. Soldatov, M. V. Ufimtsev, A. O. Urazbaev, G. Van Oost, and L. G. Zimeleva, Plasma Phys. Control. Fusion **48**, S87 (2006).
4. Z. Yan, G. R. Mckee, J. A. Boedo, D. L. Rudakov, P. H. Diamond, G. Tynan, R. J. Fonck, R. J. Groebner, T. H. Osborne, and P. Gohil, Nucl. Fusion **53**, 113038 (2013).
5. W. W. Heidbrink, E. Ruskov, E. M. Carolipio, J. Fang, M. A. van Zeeland, and R. A. James, Phys. Plasmas **6**, 1147 (1999).
6. F. Zonca and L. Chen, Europhys. Lett. **83**, 35001 (2008).
7. A. I. Smolyakov, C. Nguyen, and X. Garbet, Nucl. Fusion **50**, 054002 (2010).
8. A. I. Smolyakov, X. Garbet, G. Falchetto, and M. Ottaviani, Phys. Lett. A **372**, 6750 (2008).
9. A. V. Melnikov, L. G. Eliseev, A. V. Gudozhnik, S. E. Lysenko, V. A. Mavrin, S. V. Perfilov, L. G. Zimeleva, M. V. Ufimtsev, L. I. Krupnik, and P. M. Schoch, Czech. J. Phys. **55**, 349 (2005).
10. A. D. Gurchenko, E. Z. Gusakov, A. B. Altukhov, E. P. Selyunin, L. A. Esipov, M. Yu. Kantor, D. V. Kouprienko, S. I. Lashkul, A. Yu. Stepanov, and F. Wagner, Plasma Phys. Control. Fusion **55**, 085017 (2013).
11. T. Ido, Y. Miura, K. Kamiya, Y. Hamada, K. Hoshino, A. Fujisawa, K. Itoh, S.-I. Itoh, A. Nishizawa, H. Ogawa, Y. Kusama, and JFT-2M group, Plasma Phys. Control. Fusion **48**, S41 (2006).
12. W. Chen, X. T. Ding, L. M. Yu, X. Q. Ji, Z. B. Shi, Y. P. Zhang, W. L. Zhong, G. L. Yuan, J. Q. Dong, Q. W. Yang, Yi. Liu, L. W. Yan, Y. Zhou, M. Jiang, W. Li, X. M. Song, S. Y. Chen, X. R. Duan, and the HL-2A team, Nucl. Fusion **53**, 113010 (2013).
13. G. D. Conway, C. Tröster, B. Scott, K. Hallatschek, and the ASDEX Upgrade Team, Plasma Phys. Control. Fusion **50**, 055009 (2008).
14. C. A. de Meijere, S. Coda, Z. Huang, L. Vermare, T. Vernay, V. Vuille, S. Brunner, J. Dominski, P. Henne-

quin, A. Krämer-Flecken, G. Merlo, L. Porte, and L. Villard, Plasma Phys. Control. Fusion **56**, 072001 (2014).

15. V. V. Bulanin, F. Wagner, V. I. Varfolomeev, V. K. Gusev, G. S. Kurskiev, V. B. Minaev, M. I. Patrov, A. V. Petrov, Yu. V. Petrov, D. V. Prisyazhnyuk, N. V. Sakharov, S. Yu. Tolstyakov, N. A. Khromov, P. B. Shchegolev, and A. Yu. Yashin, Tech. Phys. Lett. **40**, 375 (2014).
16. A. V. Melnikov, L. G. Eliseev, S. A. Grashin, A. V. Gudozhnik, S. E. Lysenko, V. A. Mavrin, S. V. Perfilov, S. V. Soldatov, D. A. Shelukhin, V. A. Vershkov, L. G. Zimeleva, M. V. Ufimtsev, L. I. Krupnik, A. D. Komarov, and A. S. Kozachek, *30th EPS Conference on Plasma Physics, St. Petersburg, 2003*, Rep. P3-114; http://epsppd.epfl.ch/StPetersburg/PDF/P3_114.PDF.
17. A. V. Melnikov, C. Hidalgo, L. G. Eliseev, E. Ascasibar, A. A. Chmyga, K. S. Dyabilin, I. A. Krasilnikov, V. A. Krupin, L. I. Krupnik, S. M. Khrebtov, A. D. Komarov, A. S. Kozachek, D. Lupez-Bruna, S. E. Lysenko, V. A. Mavrin, J. L. de Pablos, I. Pastor, S. V. Perfilov, M. A. Pedrosa, R. V. Shurygin, V. A. Vershkov, T-10 team, and TJ-II team, Nucl. Fusion **51**, 083043 (2011).
18. Yu. N. Dnestrovskij, A. V. Melnikov, L. I. Krupnik, and I. S. Nedzelskij, IEEE Trans. Plasma Science **22**, 310 (1994).
19. A. V. Melnikov, I. S. Bondarenko, S. L. Efremov, N. K. Kharchev, S. M. Khrebotv, L. I. Krupnik, I. S. Nedzelskij, L. G. Zimeleva, and Yu. V. Trofimenko, Rev. Sci. Instrum. **66**, 317 (1995).
20. A. V. Melnikov, L. G. Eliseev, S. V. Perfilov, V. F. Andreev, S. A. Grashin, K. S. Dyabilin, A. N. Chudnovskiy, M. Yu. Isaev, S. E. Lysenko, V. A. Mavrin, M. I. Mikhailov, D. V. Ryzhakov, R. V. Shurygin, V. N. Zenin, and the T-10 Team, Nucl. Fusion **53**, 093019 (2013).
21. V. P. Lakhin and E. A. Sorokina, Phys. Lett. A **378**, 535 (2014).
22. V. I. Ilgisonis, I. V. Khalzov, V. P. Lakhin, A. I. Smolyakov, and E. A. Sorokina, Plasma Phys. Control. Fusion **56**, 035001 (2014).
23. R. V. Shurygin and A. A. Mavrin, Plasma Phys. Rep. **36**, 535 (2010).
24. R. V. Shurygin, Plasma Phys. Rep. **38**, 93 (2012).

Translated by L. Mosina